Coherent Wave Propagation in Multimode Systems with Correlated Noise

Yaxin Li,[1] Doron Cohen,[2] and Tsampikos Kottos[1]
[1]Wave Transport in Complex Systems Lab, Physics Department, Wesleyan University, Middletown Connecticut 06459, USA
[2]Department of Physics, Ben-Gurion University of the Negev, Beer-Sheva 84105, Israel

(Received 11 December 2018; published 18 April 2019)

Imperfections in multimode systems lead to mode mixing and interferences between propagating modes. Such disorder is typically characterized by a finite correlation time (in quantum evolution) or correlation length (in paraxial evolution). We show that the long-scale dynamics of an initial excitation that spread in mode space can be tailored by the coherent dynamics on a short scale. In particular we unveil a universal crossover from exponential to power-law ballisticlike decay of the initial mode. Our results have applications to various wave physics frameworks, ranging from multimode fiber optics to quantum dots and quantum biology.

DOI: 10.1103/PhysRevLett.122.153903

Introduction.—The prevalence of wave coherent transport in multimode systems in the presence of noisy environments is a research theme, with relevance to a range of physics frameworks. For example, in the frameworks of quantum electronics, optics or matter waves the quest to develop methods that control coherence in many-particle systems at the quantum limit has inspired new quantum computation and information technologies that are emerging of late [1–4]. Recently, in the seemingly remote field of quantum biology [5–11], researchers have also provided experimental evidence of wavelike (coherent) energy transfer in "warm, wet, and noisy" environments. A prominent example is the establishment of the important role of coherence in optimizing photosynthesis. Such findings triggered a number of tantalizing questions like the possible role of coherent (quantum) physics in brain functions, etc. It is natural, therefore, to ask whether there are universal design principles that enforce coherence dynamics in various wave transport settings where dynamical disorder (noise) cannot be ignored.

The same basic question emerges, yet, in classical wave transport in the framework of fiber optics [12]. Optical fibers have revolutionized many modern technologies ranging from medical imaging and information-transfer technologies to modern communications. Along these lines, multimode fibers (MMFs) [13–16] have recently been exploited as alternatives to single mode fibers—the latter experiencing information capacity limitations, imposed by amplifier noise and fiber nonlinearities. What makes MMFs attractive is the possibility to utilize the multiple modes as extra degrees of freedom in order to carry additional information, thus increasing the information capacity of a single fiber. On the counter side, MMF suffer from mode coupling due to external perturbations (index fluctuations and fiber bending and twisting) and from polarization scrambling effects due to fiber imperfections (core ellipticity and eccentricity, bending, etc.). Both effects cause cross talk and interference between propagating signals in different modes or polarizations. To make things worse, the fiber imperfections vary with the propagation distance z (aka quenched disorder). It is, therefore, imperative to develop theories that take into consideration the role of disorder in the modal (and polarization) mixing and provide a quantitative description of light transport in MMFs.

Outline.—We utilize a random matrix theory (RMT) approach in order to unveil a physical mechanism that shields wave coherent effects in the presence of disorder. After a short discussion of the modeling assumptions, we specifically consider a MMF that consists of N modes with propagation constants $\beta_n = n\Delta$, where $n = 1, \ldots, N$. Given an initial mode excitation (labeled n_0), the main objective is to study the decay of its survival probability $\mathcal{P}(z)$ towards the ergodic limit $\sim 1/N$. The mode mixing is due to quenched disorder associated with external perturbations along the propagation direction z of the MMF. It is characterized by its strength ε and by a correlation length z_c. From a practical as well as a physical point of view the interest is mainly in moderate disorder of strength ε, that can be characterized by a Fermi golden rule rate

$$\Gamma = \frac{4\pi}{\Delta}\varepsilon^2, \qquad (\Delta < \varepsilon < \sqrt{N}\Delta). \tag{1}$$

Consequently, we will introduce two length scales:

$$z_\Delta \equiv \frac{2\pi}{N\Delta}; \quad z_\Gamma \equiv \frac{1}{\Gamma}. \tag{2}$$

The former is the short length scale over which the bandwidth is resolved, while the latter characterizes the nonstochastic coherent decay of an excitation. We distinguish between *short* correlation length ($z_c < z_\Delta$) and *long*

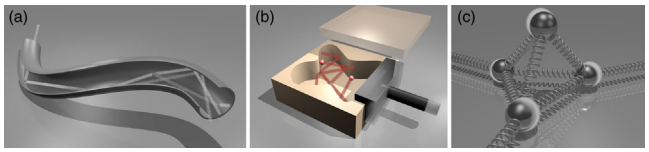

FIG. 1. Schematics of various multimode systems in the presence of a noisy environment: (a) A MMF experiencing twists, bendings, and other forms of perturbations along the propagation direction z. (b) A multimode quantum dot (or a multimode optomechanical cavity) with an incoherently moving wall. (c) Random network of coupled mechanical oscillators (slow envelope approximation) in the presence of a noisy environment.

correlation length ($z_c > z_\Gamma$). In the latter regime we discovered a ballisticlike decay $\mathcal{P}(z) \sim 1/z$ as opposed to the exponential decay for shorter z_c. The universal nature of our RMT modeling implies that our predictions are relevant for a variety of physical systems, such as multimode cavities with rough surfaces, multilevel systems with complex topology (see Fig. 1), etc. These settings can naturally emerge in areas as diverse as mesoscopic optics, microwaves and acoustics, to matter waves, quantum electronics, and quantum biology.

RMT modeling.—The RMT approach typically uncovers the most universal properties of wave transport in complex systems, and it can therefore serve as a good starting point for the understanding of designing schemes that protect the wave nature of propagation against noise or disorder. In the present context the validity of the RMT approach, including spatial and polarization degrees of freedom, is based on a paraxial approximation: see the review in Ref. [15] and some engineering-oriented publications [17,18]. The validity of the RMT modeling has been further established experimentally [19,20]. The perturbations along the propagation distance (z) of the fiber induces coupling between the N propagating modes, and therefore it is formally like the evolution in time (t) of a quantum system in N dimensional Hilbert space. Based on this formal analogy we can define the z dependent Hamiltonian H that describes the field propagation along the MMF. This Hamiltonian is represented by an $N \times N$ matrix. In the absence of disorder the unperturbed Hamiltonian $H = H_0$ is diagonal in the mode representation, with elements $H_{nm} = \beta_n \delta_{n,m}$. For simplicity we assume that the mode propagation constants are equally spaced, namely, $\beta_n = n\Delta$, where $n = 1, \ldots, N$. In practice the mode spacing can be nonuniform, but this will not affect the general conclusions that are presented below. For example, in the Supplemental Material [21] we show that a (moderate) randomization of the propagation constants has no significant effect. For simplicity of presentation we also ignore the polarization degree of freedom: we also show that its presence does not alter the general picture, apart from an abrupt 50% drop in the survival probability during the first evolution step.

The disorder.—A key observation in the analysis below is that any realistic disorder is characterized by a *finite* correlation distance. The z-dependent Hamiltonian can be written as $H = H_0 + V(z)$, where $V(z)$ is formally analogous to the time dependent potential with some correlation function $\langle V(z')V(z'')\rangle = C[(z' - z'')/z_c]$. We assume that the correlation function does not have heavy tails, and therefore, in practice, the fiber can be regarded as a chain of independent segments. Each segment has length z_c. The paraxial Hamiltonian of the kth segment $H^{(k)} = H_0 + \varepsilon B^{(k)}$ describes the field propagation under the influence of a constant perturbation $B^{(k)} = (B^{(k)})^\dagger$. The perturbation matrix is responsible for the mode mixing. The different $B^{(k)}$ can be regarded as a set of statistically independent random matrices of a Gaussian unitary ensemble (GUE). For such matrix $\langle |B|^2 \rangle = 2$; hence the off diagonal terms of the Hamiltonian have dispersion $2\varepsilon^2$ and zero average. Note that this factor of 2 is reflected in the definition of Eq. (1). The field propagation in each section k is described by the unitary matrix

$$U^{(k)} = e^{-i(H_0 + \varepsilon B^{(k)})z_c}. \tag{3}$$

The one step dynamics is characterized by a stochastic kernel

$$P(n|n_0) = \overline{|\langle n|U^{(k)}|n_0\rangle|^2} \tag{4}$$

$$\equiv (1-\lambda)\delta_{n,n_0} + \lambda W(n - n_0). \tag{5}$$

Here we averaged the one-step dynamics over realizations of the random matrix $B^{(k)}$. The parameter λ is defined as the probability that is drained from the initial mode after one step. The function $W(n - n_0)$ describes the distribution of the probability over the other modes. The modal field amplitudes $\Psi_n(z)$ at distance z along the MMF are determined by operating on the initial state $\Psi_n(0) = \delta_{n,n_0}$ with an ordered sequence of $U^{(k)}$ matrices ($k = 1, 2, \ldots$). This multistep dynamics generates a distribution $P_z(n|n_0) = |\Psi_n(z)|^2$. Below we discuss how $P_z(n|n_0)$ is related to $P(n|n_0)$, and what are the implications regrading the survival probability

$$\mathcal{P}(z) \equiv P_z(n_0|n_0). \tag{6}$$

Short correlation length.—For short segment ($z_c < z_\Delta$) the probability that is transferred to each of the N modes is $2\varepsilon^2 z_c^2$; hence the total probability that is drained from the initial mode is

$$\lambda = N \times 2\varepsilon^2 z_c^2 = \frac{z_c^2}{z_\Gamma z_\Delta}. \tag{7}$$

As long as the first term in Eq. (5) dominates, successive convolutions lead to exponential decay: After the first step

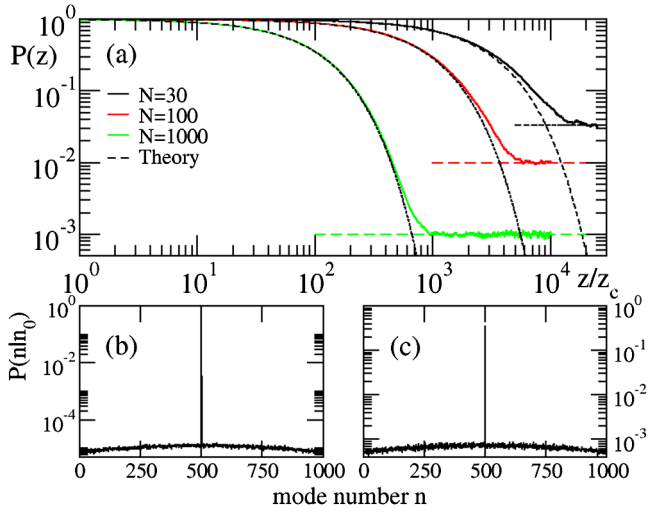

FIG. 2. (a) The decay of the survival probability for short correlation lengths $z_c = 0.005$, and perturbation strength $\varepsilon = 0.5$. The units are chosen such that $\Delta = 1$. The various colored curves indicate MMFs with different number of modes $N = 30$, 100, 1000. The colored horizontal dashed lines indicate the ergodic value $\mathcal{P}(z) \approx 1/N$. The black dashed lines indicate Eq. (8). (b) The coherent spreading $P(n|n_0)$ for $z = z_c$. (c) The spreading profile $P_z(n|n_0)$ for $z = 100z_c$.

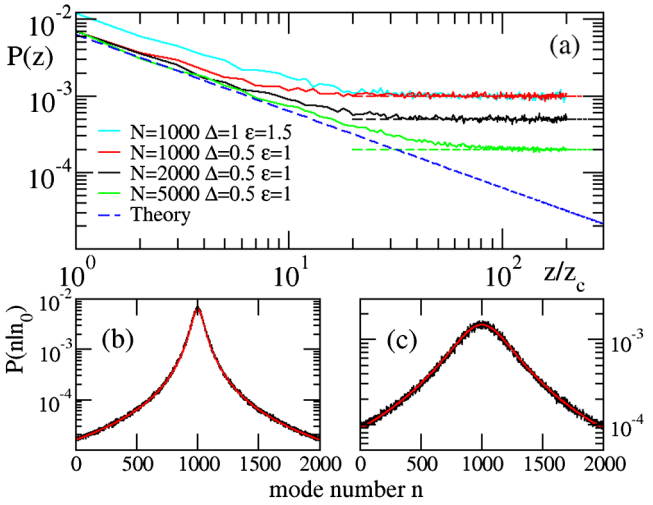

FIG. 3. (a) The decay of the survival probability for large correlation length $z_c = 0.32$. The various colored curves indicate MMFs with different parameters as indicated in the figure legend. The horizontal dashed lines indicate the ergodic limit $\mathcal{P}(z) \approx 1/N$. The blue dashed line indicates Eq. (10). (b) The coherent spreading $P(n|n_0)$ for $z = z_c$. (c) The spreading profile $P_z(n|n_0)$ for $z = 5z_c$. In both (b) and (c) the parameters are $\Delta = 0.5$, $\varepsilon = 1$, and $N = 2000$ while the red dashed line indicates the Lorentzian of Eq. (9).

the survival probability is $(1-\lambda)$, which we write as $\exp(-\tilde{\lambda})$, where for moderate disorder [see Eq. (1)] $\tilde{\lambda} \approx \lambda \ll 1$. After $t = z/z_c$ steps, if we neglect backflow, the survival probability is $\exp(-\lambda t)$. Hence,

$$\mathcal{P}(z) = \exp\left(-\frac{z_c}{z_\Delta z_\Gamma} z\right), \quad \text{for } z_c < z_\Delta. \tag{8}$$

The above has been tested numerically using RMT modeling and was found to reproduce nicely the results of our simulations for various N values, see Fig. 2(a). In the same figure we also display the single step $P(n|n_0)$, and the $P_z(n|n_0)$ distribution after 100 steps, see Figs. 2(b) and 2(c), respectively. In both instances the shape of the evolving distribution is dominated by a delta peak around the initial mode ($n_0 = N/2$). This delta peak is gradually drained, until it attains the ergodic value $\mathcal{P}(z) \approx 1/N$. Accordingly the exponential law holds as long as $\lambda t \ll \ln(N)$.

Large correlation length.—For $z_c > z_\Gamma$ it is well known from the study of the coherent dynamics [22,23] that the initial delta peak completely dissolves, and one obtains Eq. (5) with $\lambda \sim 1$ and Lorentzian line shape

$$W(n-n_0) = \frac{\Delta}{\pi} \frac{\Gamma}{[(n-n_0)\Delta]^2 + \Gamma^2}. \tag{9}$$

Recall that there is a formal analogy here with the time evolution of a quantum system under the influence of noise, where z is the time. Accordingly, Γ is the FGR rate of transitions to other levels, z_Γ of Eq. (2) is the Wigner decay time, and Eq. (9) is the Wigner Lorentzian [24]. This line shape is obtained after distance z_Γ. After a larger distance $z_c > z_\Gamma$ the line shape does not change, but the phases of the wave function are further randomized. It follows that the coherent evolution over successive segments can be approximated as a convolution of $W(n'-n'')$ kernels. We therefore get effectively stochastic evolution. But this stochastic evolution does not obey the central limit theorem. It is of the Levy-flight type because the Lorentzian does not have a finite second moment. Successive convolutions of $t = z/z_c$ Lorentzians give a wider Lorentzian of width Γt. It follows from Eq. (9) that the survival provability decays in a ballisticlike fashion:

$$\mathcal{P}(z) = 2\frac{z_\Gamma z_c}{N z_\Delta}\frac{1}{z}, \quad \text{for } z_c > z_\Gamma. \tag{10}$$

The above picture is nicely confirmed by our numerical analysis using RMT modeling. In Fig. 3(a) we report our findings for the survival probability for various mode sizes N, and perturbation strengths ε. In Fig. 3(b) we also report the Lorentzian waveform at the end of the coherent evolution $z = z_c$. The robustness of the Lorentzian shape Eq. (9) against the dynamical disorder is further confirmed in Fig. 3(c) where we plot $P_z(n|n_0)$ after 5 segments.

Intermediate correlation length.—Consider $z_\Delta < z_c < z_\Gamma$. In this case, the initial spreading is dictated by a Fermi golden rule (FGR) type picture. Namely, the probability that is transferred to each of the modes within the

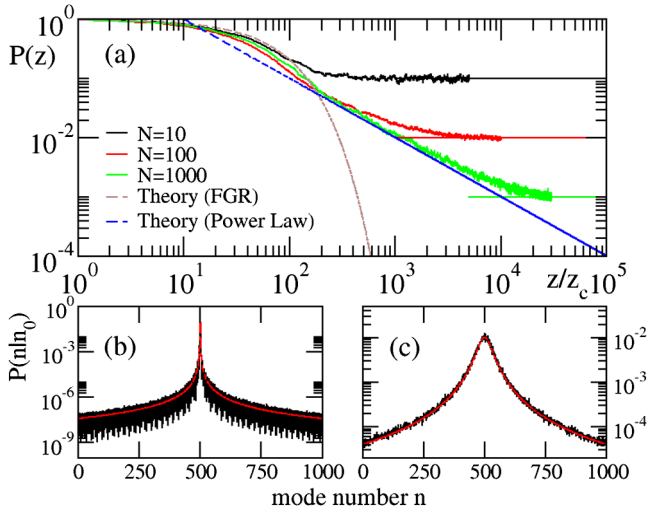

FIG. 4. (a) The decay of the survival probability for intermediate correlation length $z_c = 1$, and perturbation strength $\varepsilon = 0.05$. The units are chosen such that $\Delta = 1$. The various colored curves indicate MMFs with different numbers of modes $N = 10, 100, 1000$. The colored horizontal dashed lines indicate the ergodic limit $\mathcal{P}(z) \approx 1/N$. The brown dashed line indicates the FGR exponential decay Eq. (12), while the blue dashed line indicates the power-law decay Eq. (10). (b) The coherent spreading $P(n|n_0)$ for $z = z_c$. (c) The spreading profile $P_z(n|n_0)$ for $z = 1000 z_c$. In both (b) and (c) the parameters are $\Delta = 1$, $\varepsilon = 0.05$, and $N = 1000$ while the red dashed line indicates the Lorentzian of Eq. (9).

unresolved bandwidth $2\pi/z_c$ is $(\varepsilon z_c)^2$; hence the total probability that is drained from the initial mode is

$$\lambda = \Gamma z_c. \tag{11}$$

The analysis proceeds as in the discussion of the short correlation scale, just with this different expression for λ. Namely, as long as the first term in Eq. (5) dominates, successive convolutions lead to exponential decay $\exp(-\lambda t)$ with $t = z/z_c$. Consequently, we obtain a result that is independent of z_c, namely,

$$\mathcal{P}(z) = \exp\left[-\frac{1}{z_\Gamma} z\right], \quad \text{for } z_\Delta < z_c < z_\Gamma. \tag{12}$$

Equation (12) compares nicely with the numerical simulations using RMT modeling, see Fig. 4(a). Notice that as opposed to Eq. (8), now the decay rate does not involve the number of modes of the system N and neither depends on z_c. At the same time the envelope of the evolving waveform acquires Lorentzian-like tails spilled all over the N modes, see Fig. 4(b). Nevertheless, the dominant component of the waveform is centered at the initial mode n_0. For larger propagation distances $z > z_\Gamma$, the FGR decay law Eq. (12) ceases to apply. Instead, either the waveform reaches an ergodic distribution [see the black line in Fig. 4(a), corresponding to $N = 10$] or (in the case of large number of modes N) it continues spreading, albeit with a different form. Specifically, the previous argument associated with the robustness of the Lorentzian waveform against noise takes over, and we recover the physics that led us to Eqs. (9), (10), see Figs. 4(a), 4(c).

Strong disorder, diffusive decay.—So far we have discussed weak disorder. We now turn to discuss briefly the strong disorder regime ($\varepsilon > \sqrt{N}\Delta$). The scenario for short z_c is formally the same as that of the "short correlation" analysis, leading to an exponential decay. But if z_c exceeds $z_N = 1/(\sqrt{N}\varepsilon)$ the probability is drained from the initial mode, and the distribution becomes ergodic with $\mathcal{P}(z) \approx 1/N$. At this stage one wonders why the naively expected diffusive decay does not appear. Are we missing something in the analysis? The answer is that the analysis so far has assumed B that looks like a full GUE matrix. But in a more general circumstance B might have a finite bandwidth $b \ll N$. The analysis for the weak disorder regime still holds but with N replaced by b. In contrast, in the strong disorder regime, it is well known [22] that the saturation profile is not a Lorentzian. Rather, if z_c is long enough, the saturation profile is exponentially localized over $\xi = b^2$ modes. Such a saturation profile has a finite second moment. Consequently, the same argumentation as in the "long correlation regime" implies that the width of the distribution evolves as $\xi\sqrt{t}$, where $t = z/z_c$ is the number of steps. This leads to the conclusion that the survival provability decays in a diffusivelike fashion:

$$\mathcal{P}(z) \approx \frac{1}{b^2}\sqrt{\frac{z_c}{z}}. \tag{13}$$

Because of lack of space, we defer a more detailed discussion of other results and a thorough analysis of the decay of the survival probability for the more realistic case where $b \ll N$ to a later publication [25].

Summary.—We have illuminated the interplay between the short time coherent evolution and the longtime stochastic spreading in multimode systems. The correlation scale z_c of a disordered environment determines the crossover from an exponential decay to diffusivelike or ballisticlike decay. The latter is due to a Levy-type spreading which is implied by convolution of Lorentzian kernels. We would like to highlight, once again, the novelty of the analysis of the large correlation length regime, leading to Eq. (10). It delivers the message that Levy-flight type dynamics is generically expected once the finite correlation of the disorder is taken into account. This should be contrasted with the exponential decay in the FGR regime (for intermediate correlation scale), which is demonstrated for the first time in the present context, but it is not novel in the traditional quantum context of time dependent dynamics. Our results have been formulated using a universal RMT modeling. A future direction that we currently pursue [25] is to design

other coupling schemes for which the one-step coherent evolution leads to tailored anomalous decay of the survival probability.

Y. L. and T. K. acknowledge partial support by an AFOSR Grant No. FA9550-14-1-0037, and by an NSF Grant No. EFMA-1641109. Y. L. acknowledges funding from the Wesleyan University CIS summer research program. D. C. acknowledges support by the Israel Science Foundation (Grant No. 283/18). The authors acknowledge useful discussions with E. Makri and Y. Cai who participated at the initial stage of the project.

[1] K. Southwell, Quantum coherence, Nature (London) **453**, 1003 (2008) and articles therein.
[2] J. P. Dowling and G. J. Milburn, Quantum technology: The second quantum revolution, Phil. Trans. R. Soc. A **361**, 1655 (2003).
[3] E. Andersson and P. Öhberg, *Quantum Information and Coherence* (Springer, New York, 2014).
[4] D. V. Averin, B. Ruggiero, and P. Silvertrini, *Macroscopic Quantum Coherence and Quantum Computing* (Springer, New York, 2001).
[5] G. S. Engel, T. R. Calhoun, E. L. Read, T.-K. Ahn, T. Mancal, Y.-C. Cheng, R. E. Blankenship, and G. R. Fleming, Evidence for wavelike energy transfer through quantum coherence in photosynthetic systems, Nature (London) **446**, 782 (2007).
[6] G. Panitchayangkoona, D. Hayesa, K. A. Fransteda, J. R. Carama, E. Harela, J. Wenb, R. E. Blankenshipb, and G. S. Engela, Long-lived quantum coherence in photosynthetic complexes at physiological temperature, Proc. Natl. Acad. Sci. U.S.A. **107**, 12766 (2010).
[7] M. Sarovar, A. Ishizaki, G. R. Fleming, and K. B. Whaley, Quantum entanglement in photosynthetic light-harvesting complexes, Nat. Phys. **6**, 462 (2010).
[8] S. Lloyd, Quantum coherence in biological systems, J. Phys. Conf. Ser. **302**, 012037 (2011).
[9] G. S. Engel, Quantum coherence in photosynthesis, Procedia Chem. **3**, 222 (2011).
[10] G. R. Fleming, G. D. Scholes, and Y.-C. Cheng, Quantum effects in biology, Procedia Chem. **3**, 38 (2011).
[11] Y. Zhang, G. L. Celardo, F. Borgonovi, and L. Kaplan, Opening-assisted coherent transport in the semiclassical regime, Phys. Rev. E **95**, 022122 (2017).
[12] G. Keiser, *Optical Fiber Communications*, 3rd ed. (McGraw-Hill, New York, 2000).
[13] B. Redding, M. Alam, M. Seifert, and H. Cao, High-resolution and broadband all-fiber spectrometers, Optica **1**, 175 (2014).
[14] W. Xiong, P. Ambichl, Y. Bromberg, B. Redding, S. Rotter, and H. Cao, Spatiotemporal Control of Light Transmission through a Multimode Fiber with Strong Mode Mixing, Phys. Rev. Lett. **117**, 053901 (2016).
[15] K.-P. Ho and J. M. Kahn, Mode coupling and its impact on spatially multiplexed systems, *Optical Fiber Telecommunications VIB* (Elsevier, New York, 2013).
[16] W. Xiong, P. Ambichl, Y. Bromberg, B. Redding, S. Rotter, and H. Cao, Principal modes in multimode fibers: Exploring the crossover from weak to strong mode coupling, Opt. Express **25**, 2709 (2017).
[17] M. B. Shemirani, W. Mao, R. A. Panicker, and J. M. Kahn, Principal modes in graded-index multimode fiber in presence of spatial- and polarization-mode coupling, J. Lightwave Technol. **27**, 1248 (2009).
[18] K.-P. Ho and J. M. Kahn, Statistics of group delays in multimode fiber with strong mode coupling, J. Lightwave Technol. **29**, 3119 (2011).
[19] P. Chiarawongse, H. Li, W. Xiong, C. W. Hsu, H. Cao, and T. Kottos, Statistical description of transport in multimode fibers with mode-dependent loss, New J. Phys. **20**, 113028 (2018).
[20] W. Xiong, C. W. Hsu, Y. Bromberg, J. E. Antonio-Lopez, R. A. Correa, and H. Cao, Complete polarization control in multimode fibers with polarization and mode coupling, Light Sci. Appl. **7**, 54 (2018).
[21] See Supplemental Material at http://link.aps.org/supplemental/10.1103/PhysRevLett.122.153903 for a numerical simulation that demonstrates the implications of random mode spacing. This randomness is reflected only if the disorder is very weak ($\epsilon < \Delta$). See also a numerical simulation that takes into account that there are two sets of modes due to the polarization degree of freedom. The main implication is a quick 50% drop at the initial time due to the randomization of the polarization direction.
[22] D. Cohen, F. M. Izrailev, and T. Kottos, Wave Packet Dynamics in Energy Space, Random Matrix Theory, and the Quantum-Classical Correspondence, Phys. Rev. Lett. **84**, 2052 (2000).
[23] J. L. Gruver, J. Aliaga, H. A. Cerdeira, P. Mello, and A. N. Proto, Energy-level statistics and time relaxation in quantum systems, Phys. Rev. E **55**, 6370 (1997).
[24] D. Cohen and T. Kottos, Parametric dependent Hamiltonians, wave functions, random matrix theory, and quantal-classical correspondence, Phys. Rev. E **63**, 036203 (2001).
[25] Y. Li, D. Cohen, and T. Kottos (in preparation).